Macroscopic Dark Matter Detection Using Fluorescence Detectors

Jagjit Singh Sidhu, Roshan Abraham, Glenn Starkman, Corbin Covault

Case Western Reserve University

Pheno 2018
8th May 2018

Introduction

- Several different lines of evidence point to the existence of dark matter(e.g. rotation curves, bullet cluster etc.).

Introduction

- Several different lines of evidence point to the existence of dark matter(e.g. rotation curves, bullet cluster etc.).
- A wide variety of dark matter candidates have been explored in recent times(due to various reasons).

Introduction

- Several different lines of evidence point to the existence of dark matter(e.g. rotation curves, bullet cluster etc.).
- A wide variety of dark matter candidates have been explored in recent times(due to various reasons).
- We consider a broad class of macroscopic dark matter candidates, with characteristic size(cross section) in cm^2 and mass in g.

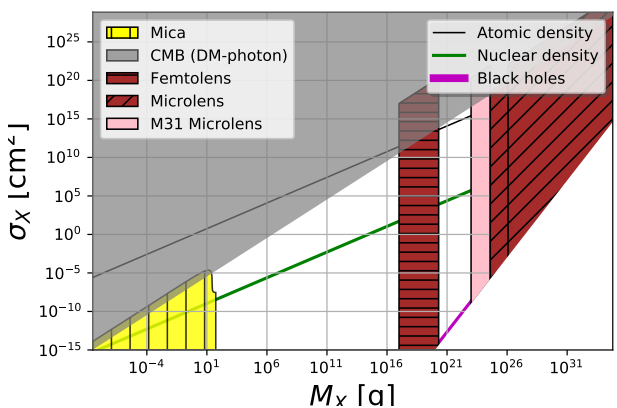

Fluorescence

- A general detection scheme has been developed for measuring the fluorescence caused by a passing macro in the atmosphere.

Fluorescence

- A general detection scheme has been developed for measuring the fluorescence caused by a passing macro in the atmosphere.
- We propagate the initial energy deposition by the macro to obtain the area at time t that reaches a particular state of ionization I

$$\pi r_I(t)^2 = 4\pi\alpha t \log\left(\frac{\sigma_x v_x^2}{4\pi\alpha t c_p T_I}\right). \tag{1}$$

Fluorescence

- A general detection scheme has been developed for measuring the fluorescence caused by a passing macro in the atmosphere.
- We propagate the initial energy deposition by the macro to obtain the area at time t that reaches a particular state of ionization I

$$\pi r_I(t)^2 = 4\pi\alpha t \log\left(\frac{\sigma_x v_x^2}{4\pi\alpha t c_p T_I}\right). \tag{1}$$

- For large enough r_I, the plasma becomes optically thick. Macros with $\sigma_x \gtrsim 10^{-7} cm^2$ will produce an optically thick plasma that will radiate as a blackbody.

Photon production in the optically thin regime

- For the optically thin scenario, we solve the Boltzmann equation ignoring any cooling terms giving the number of photons produced per unit length along the macro path trajectory

$$\frac{\mathrm{d}N}{\mathrm{d}l} = 2\eta\pi \sum_I \int_0^{t_{I0}} \int_0^{r_I(t)} \beta_I n_{eI} n_a \alpha_{rad} r dr dt \tag{2}$$

Photon production in the optically thin regime

- For the optically thin scenario, we solve the Boltzmann equation ignoring any cooling terms giving the number of photons produced per unit length along the macro path trajectory

$$\frac{\mathrm{d}N}{\mathrm{d}l} = 2\eta\pi \sum_I \int_0^{t_{I0}} \int_0^{r_I(t)} \beta_I n_{eI} n_a \alpha_{rad} r dr dt \tag{2}$$

- The number of photons received in a detector pixel in one bin time is

$$N_\gamma^{thin} \simeq 7 \times 10^{27} \frac{A_{detector} \sin\theta}{D\ km} \left(\frac{\sigma_x}{cm^2}\right)^2 . \tag{3}$$

Photon production in the optically thin regime

- For the optically thin scenario, we solve the Boltzmann equation ignoring any cooling terms giving the number of photons produced per unit length along the macro path trajectory

$$\frac{\mathrm{d}N}{\mathrm{d}l} = 2\eta\pi \sum_I \int_0^{t_{I0}} \int_0^{r_I(t)} \beta_I n_{eI} n_a \alpha_{rad} r dr dt \tag{2}$$

- The number of photons received in a detector pixel in one bin time is

$$N_\gamma^{thin} \simeq 7 \times 10^{27} \frac{A_{detector} \sin\theta}{D\ km} \left(\frac{\sigma_x}{cm^2}\right)^2 . \tag{3}$$

- The numerical prefactor is now solely a detector dependent quantity.

Photon production in the optically thick regime

- We integrate the Planck spectrum to find the number of photons emitted by the plasma per unit length along the macro trajectory

$$\frac{\mathrm{d}N}{\mathrm{d}l} = \int_0^{t_{cool}} \int_{\nu_{350nm}}^{\nu_{400nm}} \frac{4\pi 2\pi r_{10000K}(t)}{h\nu} B(\nu, T) d\nu dt \qquad (4)$$

Photon production in the optically thick regime

- We integrate the Planck spectrum to find the number of photons emitted by the plasma per unit length along the macro trajectory

$$\frac{\mathrm{d}N}{\mathrm{d}l} = \int_0^{t_{cool}} \int_{\nu_{350nm}}^{\nu_{400nm}} \frac{4\pi 2\pi r_{10000K}(t)}{h\nu} B(\nu, T) d\nu dt \qquad (4)$$

- We get N_γ^{thick} just as in the free-streaming case

Photon production in the optically thick regime

- We integrate the Planck spectrum to find the number of photons emitted by the plasma per unit length along the macro trajectory

$$\frac{\mathrm{d}N}{\mathrm{d}l} = \int_0^{t_{cool}} \int_{\nu_{350nm}}^{\nu_{400nm}} \frac{4\pi 2\pi r_{10000K}(t)}{h\nu} B(\nu, T) d\nu dt \qquad (4)$$

- We get N_γ^{thick} just as in the free-streaming case
- The solutions do not smoothly transition at $\sigma_x = 10^{-7}\mathrm{cm}^2$. Thus, we interpolated the optically thin solution at $\sigma_x = 10^{-7}\mathrm{cm}^2$ with the optically thick solution at $\sigma_x = 9 \times 10^{-7}\mathrm{cm}^2$.

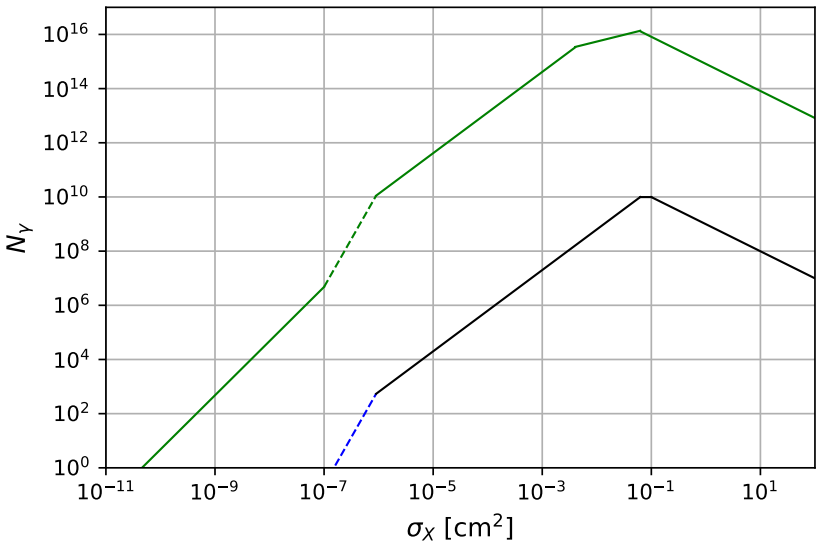

Figure 1: Number of photons received at the detector, N_γ as a function of the macro cross section for Auger in green and JEM-EUSO in black.

Specific Examples: Auger

- The Pierre Auger Observatory includes 24 FD telescopes designed to look for relativistic cosmic ray particles. Macros would move at 0.001c and so we would need to rescale the time bin. These detectors have an effective area of 120km^2.

Specific Examples: Auger

- The Pierre Auger Observatory includes 24 FD telescopes designed to look for relativistic cosmic ray particles. Macros would move at 0.001c and so we would need to rescale the time bin. These detectors have an effective area of 120km^2.
- The expected number of events for such a detector

$$N_{events}^{1FD} = 2\frac{g}{M_x}\left(\frac{D_{max}(\sigma_x)}{km}\right)^2 . \tag{5}$$

where $D_{max}(\sigma_x)$ represents the maximum distance away we could detect a macro of a particular cross section. This gives us a limit on the upper mass M_x of 660g that we could hope to probe.

Specific Examples: Auger

- The Pierre Auger Observatory includes 24 FD telescopes designed to look for relativistic cosmic ray particles. Macros would move at 0.001c and so we would need to rescale the time bin. These detectors have an effective area of 120km^2.
- The expected number of events for such a detector

$$N_{events}^{1FD} = 2\frac{g}{M_x}\left(\frac{D_{max}(\sigma_x)}{km}\right)^2 . \tag{5}$$

  where $D_{max}(\sigma_x)$ represents the maximum distance away we could detect a macro of a particular cross section. This gives us a limit on the upper mass M_x of 660g that we could hope to probe.
- If the entire Auger FD array could be used, the effective target area becomes $3 \times 10^3 km^2$. This pushes the upper mass accessible to 1.6×10^4g.

Specific Examples: Auger

- To constrain the cross section, we compare N_γ with N_{noise}

Specific Examples: Auger

- To constrain the cross section, we compare N_γ with N_{noise}
- This gives a relationship between the D_{max} and σ_x

$$D_{max}^{1FD}(\sigma_x) \quad = \quad \min\left(20, 4 \times 10^{17} \left(\frac{\sigma_x}{cm^2}\right)^2\right) km \tag{6}$$

where the upper bound of 20 km is experimentally determined by Auger.

Specific Examples: Auger

- To constrain the cross section, we compare N_γ with N_{noise}
- This gives a relationship between the D_{max} and σ_x

$$D_{max}^{1FD}(\sigma_x) \quad = \quad \min\left(20, 4 \times 10^{17} \left(\frac{\sigma_x}{cm^2}\right)^2\right) km \tag{6}$$

where the upper bound of 20 km is experimentally determined by Auger.

- For a single FD telescope we use (5) and (6) to find

$$\left(\frac{\sigma_x}{cm^2}\right)_{1FD} \geq 1 \times 10^{-9} \left(\frac{M_x}{g}\right)^{\frac{1}{4}}. \tag{7}$$

Specific Examples: Auger

- To constrain the cross section, we compare N_γ with N_{noise}
- This gives a relationship between the D_{max} and σ_x

$$D_{max}^{1FD}(\sigma_x) \quad = \quad \min\left(20, 4 \times 10^{17} \left(\frac{\sigma_x}{cm^2}\right)^2\right) km \tag{6}$$

where the upper bound of 20 km is experimentally determined by Auger.

- For a single FD telescope we use (5) and (6) to find

$$\left(\frac{\sigma_x}{cm^2}\right)_{1FD} \geq 1 \times 10^{-9} \left(\frac{M_x}{g}\right)^{\frac{1}{4}}. \tag{7}$$

- For the full Auger FD array, the lower boundary is of the same form as (7), with a slightly enhanced sensitivity to the cross section.

Specific Examples: Auger

- To constrain the cross section, we compare N_γ with N_{noise}
- This gives a relationship between the D_{max} and σ_x

$$D_{max}^{1FD}(\sigma_x) \quad = \quad \min\left(20, 4 \times 10^{17} \left(\frac{\sigma_x}{cm^2}\right)^2\right) km \tag{6}$$

where the upper bound of 20 km is experimentally determined by Auger.

- For a single FD telescope we use (5) and (6) to find

$$\left(\frac{\sigma_x}{cm^2}\right)_{1FD} \geq 1 \times 10^{-9} \left(\frac{M_x}{g}\right)^{\frac{1}{4}}. \tag{7}$$

- For the full Auger FD array, the lower boundary is of the same form as (7), with a slightly enhanced sensitivity to the cross section.
- Utilizing the entire array gives a bigger detector so we can probe to lower cross sections than with just one detector.

Specific Examples: JEM-EUSO

- JEM-EUSO is a planned Ultra-High Energy Cosmic Ray (UHECR, $E > 10^{18}$eV) detector to be placed in the Japanese Experiment Module of the International Space Station.

Specific Examples: JEM-EUSO

- JEM-EUSO is a planned Ultra-High Energy Cosmic Ray (UHECR, $E > 10^{18}$eV) detector to be placed in the Japanese Experiment Module of the International Space Station.
- JEM-EUSO will also be able to operate in "tilt" mode, looking not straight down at the Earth but at an angle to the nadir. This will increase the target area markedly and hence the upper mass that we can probe.

Specific Examples: JEM-EUSO

- JEM-EUSO is a planned Ultra-High Energy Cosmic Ray (UHECR, $E > 10^{18}$eV) detector to be placed in the Japanese Experiment Module of the International Space Station.
- JEM-EUSO will also be able to operate in "tilt" mode, looking not straight down at the Earth but at an angle to the nadir. This will increase the target area markedly and hence the upper mass that we can probe.
- We repeated the analysis for JEM-EUSO and found that $\sigma_x \geq 6 \times 10^{-7}\text{cm}^2$.

Results

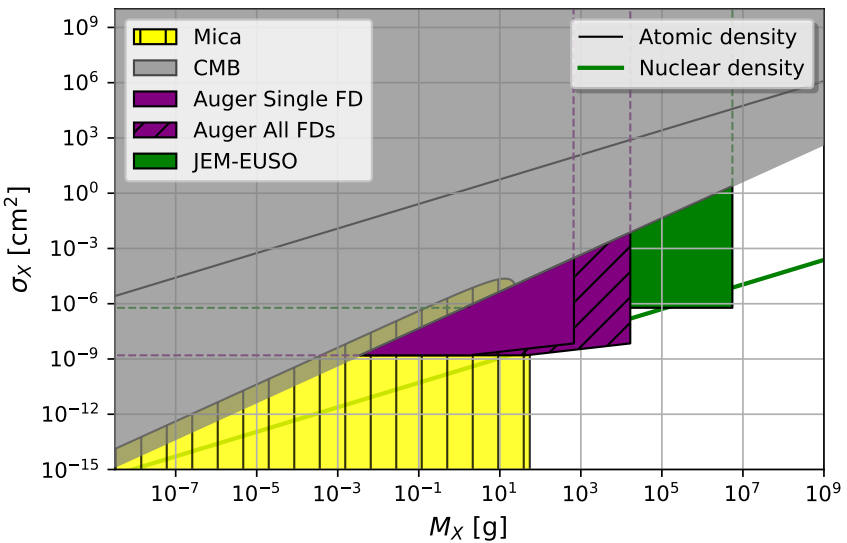

Figure 2: The parameter space that could be probed by both PA(for one FD telescope in purple and the full array in purple with diagonal lines) and JEM-EUSO(in green).

Conclusions

- Macroscopic dark matter is a broad class of alternatives to particulate dark matter that include, compelling, Standard Model Candidates.

Conclusions

- Macroscopic dark matter is a broad class of alternatives to particulate dark matter that include, compelling, Standard Model Candidates.
- The passage of a Macro through Earth's atmosphere will cause dissociation and ionization of air molecules, resulting, through recombination, in a signal visible to Fluorescence Detectors such as those used to search for Ultra High Energy Cosmic Rays.

Conclusions

- Macroscopic dark matter is a broad class of alternatives to particulate dark matter that include, compelling, Standard Model Candidates.
- The passage of a Macro through Earth's atmosphere will cause dissociation and ionization of air molecules, resulting, through recombination, in a signal visible to Fluorescence Detectors such as those used to search for Ultra High Energy Cosmic Rays.
- It is of particular significance that both detectors are sensitive to macros of nuclear or lower density, since the expected Standard Model macro candidates, as well as most others that have been explored (excepting primordial black holes), are expected to be of approximately nuclear density.